Environmental Science & Technology

Article

pubs.acs.org/est

Transformation Pathways of the Recalcitrant Pharmaceutical Compound Carbamazepine by the White-Rot Fungus *Pleurotus ostreatus*: Effects of Growth Conditions

Naama Golan-Rozen,[†,‡] Bettina Seiwert,[§] Christina Riemenschneider,[§] Thorsten Reemtsma,[§] Benny Chefetz,[†,‡] and Yitzhak Hadar*[,†]

[†]Faculty of Agriculture, Food and Environment and [‡]Center of Excellence in Agriculture and Environmental Health, The Hebrew University of Jerusalem, P.O. Box 12, Rehovot 76100, Israel

[§]Department of Analytical Chemistry, Helmholtz Centre for Environmental Research − UFZ, Permoserstrasse 15, 04318 Leipzig, Germany

Supporting Information

ABSTRACT: The widely used anticonvulsant pharmaceutical carbamazepine is recalcitrant in many environmental niches and thus poses a challenge in wastewater treatment. We followed the decomposition of carbamazepine by the white-rot fungus *Pleurotus ostreatus* in liquid culture compared to solid-state fermentation on lignocellulosic substrate where different enzymatic systems are active. Carbamazepine metabolites were identified using liquid chromatography−high-resolution mass spectrometry (LC-Q-TOF-MS). In liquid culture, carbamazepine was only transformed to 10,11-epoxy carbamazepine and 10,11-dihydroxy carbamazepine as a dead-end product. During solid-state fermentation, carbamazepine metabolism resulted in the generation of an additional 22 transformation products, some of which are toxic. Under solid-state-fermentation conditions, 10,11-epoxy carbamazepine was further metabolized via acridine and 10,11-dihydroxy carbamazepine pathways. The latter was further metabolized via five subpathways. When ^{14}C-carbonyl-labeled carbamazepine was used as the substrate, ^{14}C-CO_2 release amounted to 17.4% of the initial radioactivity after 63 days of incubation. The proposed pathways were validated using metabolites (10,11-epoxy carbamazepine, 10,11-dihydroxy carbamazepine, and acridine) as primary substrates and following their fate at different time points. This work highlights the effect of growth conditions on the transformation pathways of xenobiotics. A better understanding of the fate of pollutants during bioremediation treatments is important for establishment of such technologies.

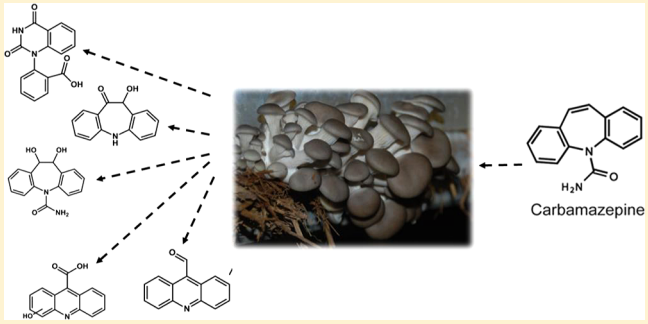

INTRODUCTION

White-rot fungi are capable of degrading lignin, a complex natural macromolecule, via unique extracellular, nonspecific oxidative systems participating in the enzymatic "combustion" of wood, using molecular oxygen as the terminal electron acceptor.[1,2] The major enzymes involved in lignin degradation are lignin peroxidase, manganese peroxidase, versatile peroxidase, and laccase.[3] Because of their unique features, the ligninolytic enzymes can also react with xenobiotics; they have been shown to facilitate the degradation and transformation of organic pollutants such as polycyclic aromatic hydrocarbons, azo-dyes, pesticides, and pharmaceuticals.[4] These compounds can be transformed by white-rot fungi via either cometabolism or catabolism.[5]

Dissipation of the recalcitrant pharmaceutical compound carbamazepine (CBZ) by fungi of different taxonomic groups has been reported.[6−10] However, only a few studies have identified the transformation products (TPs), and none of them have suggested transformation pathways. Pure liquid cultures of *Cunninghamella elegans* and *Umbelopsis ramanniana* have been shown to transform up to ∼40% of added CBZ (237 mg L^{-1}) to 2-hydroxy carbamazepine (2-OH-CBZ), 3-OH-CBZ, and 10,11-epoxy carbamazepine (EP-CBZ).[11] Pure liquid cultures of *Trametes versicolor* have been reported to remove 80% of the added CBZ (10 mg L^{-1}) during a Fenton-like reaction, and hydroxylated CBZ species were identified.[12] Jelic et al.[13] demonstrated the formation of EP-CBZ, 10,11-dihydroxy carbamazepine (*trans*-diOH-CBZ), acridine, and acridone by *T. versicolor* grown in an air-pulsed fluidized-bed bioreactor. Several other studies have demonstrated dissipation of CBZ by crude or pure lignin-modifying enzymes.[14−16] In a previous study, we have shown that the white-rot fungus *Pleurotus ostreatus* can transform CBZ at environmentally relevant

Received: May 4, 2015
Revised: July 30, 2015
Accepted: August 13, 2015
Published: September 29, 2015

DOI: 10.1021/acs.est.5b02222
Environ. Sci. Technol. 2015, 49, 12351−12362

concentrations (1 μg L^{-1}) and that two families of enzymes are involved in the process: manganese peroxidase in a Mn^{2+}-dependent or -independent manner and cytochrome P-450. In this system, EP-CBZ was the main metabolite formed, and it accumulated in the medium during the incubation period.[17] Cytochrome P-450 was also shown to be involved in the transformation of CBZ by other fungi[7] and in the oxidation of other aromatic pollutants such as polycyclic aromatic hydrocarbons.[4]

The ligninolytic system of *P. ostreatus* consists of manganese peroxidases and laccases. The former exhibit a typical peroxidase catalytic cycle with Mn^{2+} as the substrate. They can oxidize phenolic structures to phenoxy radicals, which then undergo a variety of reactions including polymer cleavage.[18] In contrast, versatile peroxidases can also oxidize nonphenolic substrates in the absence of Mn^{2+} ions.[19,20] Laccases catalyze the one-electron oxidation of phenolic, aromatic amines and other electron-rich substrates, also resulting in the formation of phenoxy radicals.[21] The ligninolytic enzymes of *P. ostreatus* are also expressed and active when the fungus is grown in synthetic medium, but when *P. ostreatus* is grown on natural lignocellulosic substrate under solid-state fermentation, the fungal physiology and enzymatic profile are tuned toward lignin degradation.[22,23] Thus, we hypothesized that growing the fungus under these conditions would facilitate degradation of the recalcitrant pharmaceutical CBZ that exhibits a chemical structure similar to that of lignin subunits. As a universal detoxification mechanism, one or more of the cytochrome P-450 gene family members are expressed and active regardless of the growth medium type. It is expected that EP-CBZ will be formed under these conditions as a result of both cytochrome P-450 and MnP/VP activities. However, as the oxidation of CBZ and metabolites by the ligninolytic system might be nonspecific, additional TPs produced downstream could resemble those of abiotic oxidizing agents.[24−28] In this study, we elucidated the transformation pathways of CBZ by *P. ostreatus* grown in rich liquid medium and during solid-state fermentation on cotton stalks.

EXPERIMENTAL SECTION

Chemicals. Carbamazepine (CBZ; 5H-dibenzo[b,f]azepine-5-carboxamide, 98%), 10,11-epoxy carbamazepine (EP-CBZ; 1a,10b-dihydro-6H-dibenzo(b,f)oxireno[d]azepine-6-carboxamide, ≥ 98%) and acridine (dibenzo[b,e]pyridine, 97%) were purchased from Sigma-Aldrich (Rehovot, Israel). rac *trans*-10,11-Dihydro-10,11-dihydroxy carbamazepine (*trans*-diOH-CBZ, 5*H*-dibenz[*b*,*f*]azepine-5-carboxamide, 10,11-dihydro-10,11-dihydroxy-, (10*R*,11*R*)-*rel*-, ≥ 97%) was purchased from Santa Cruz Biotechnology (Dallas, TX, USA). D_2-^{13}C-labeled CBZ and D_2-^{13}C-labeled EP-CBZ (Toronto Research Chemicals, Ontario, Canada) were used as internal standards for LC−MS analysis. ^{14}C-carbonyl-labeled CBZ (20 mCi $mmol^{-1}$, radiochemical and chemical purity >99%; see Figure S1 for ^{14}C-labeling position) was purchased from American Radiolabeled Chemicals (St. Louis, MO, USA).

Fungal Strains and Culture Conditions. *P. ostreatus* strain PC9 (Spanish Type Culture Collection accession number CECT20311), which is a monokaryotic derivative of the dikaryon commercial strain Florida N001 (Spanish Type Culture Collection accession number CECT20600),[29] was used throughout this study. Cultures were grown and maintained in 9 cm diameter Petri dishes containing glucose peptone (GP) medium (20 g L^{-1} glucose, 5 g L^{-1} peptone, 2 g L^{-1} yeast extract, 1 g L^{-1} K_2HPO_4, and 0.5 g L^{-1} $MgSO_4 \cdot 7H_2O$) solidified with 1.5% (w/v) agar.

Liquid cultures were incubated at 28 °C in the dark in stationary 250 mL Erlenmeyer flasks containing 50 mL of GP medium and closed with paper stoppers. The inoculum for the liquid cultures consisted of two disks (5 mm in diameter) of mycelium collected from a colony that was freshly grown in solid culture. Liquid cultures of *P. ostreatus* were incubated for 10 days; then, the medium was decanted and replaced with fresh medium containing 37 nmol mL^{-1} (8.8 mg L^{-1}) CBZ, 42 nmol mL^{-1} (10.8 mg L^{-1}) EP-CBZ, or 39.2 nmol mL^{-1} (10.6 mg L^{-1}) *trans*-diOH-CBZ per flask for an additional 25 days. Two types of controls were used: inoculated cultures without substrate and uninoculated flasks containing the substrate. Each treatment was performed in three replicates. The media were sampled twice a week to quantify residual CBZ and its metabolites.

Solid-state fermentation was conducted in 100 mL Erlenmeyer flasks using cotton stalks as the substrate. The cotton stalks were obtained from a cotton field after defoliation and harvest; the stalks were ground to <5 mm size using a Wiley mill. Cotton stalks (2 g) were weighed into the Erlenmeyer flasks, moisturized with 4 mL of ultrapure water, and autoclaved for 60 min. Samples were then incubated at 28 °C in the dark for 24 h and autoclaved again for 20 min. Aqueous solutions of CBZ, EP-CBZ, or *trans*-diOH-CBZ were freshly prepared and filtered through a sterile 0.2 μm Teflon filter, and 4 mL aliquots were added separately to the cotton stalks to a final concentration of 110 nmol g^{-1} (0.025 mg g^{-1}) CBZ, 100 nmol g^{-1} (0.02 mg g^{-1}) EP-CBZ, 95 nmol g^{-1} (0.015 mg g^{-1}) *trans*-diOH-CBZ, or 85 nmol g^{-1} (0.015 mg g^{-1}) acridine per flask. The inoculum was one disk (5 mm diameter) of mycelium obtained from the edge of a young colony grown on solid GP medium. Cultures were incubated at 28 °C in the dark for 60 days. Two types of controls were used: inoculated without substrate and uninoculated with substrate. Each treatment was performed in three replicates.

^{14}C-CBZ mineralization during solid-state fermentation was performed according to Salame et al.[30] using biometric flasks. A spiking solution of ^{14}C-CBZ was prepared by mixing 6.25 μL of the labeled CBZ with 4 mL of aqueous solution of nonlabeled CBZ (12.5 mg L^{-1}) and added to each of four replicates containing 2 g of cotton stalks. Final radioactivity was 0.625 μCi in each flask. $^{14}CO_2$ evolved in each flask was trapped in NaOH every 3−4 days for 63 days.

Extraction Procedure and Sample Preparation. Glucose peptone medium samples were filtered through a 0.2 μm Teflon filter, and 100 μL of the filtered sample was diluted with 880 μL of ultrapure water. Then, 10 μL of each internal standard solution (D_2-^{13}C-labeled CBZ and D_2-^{13}C-labeled EP-CBZ; 2 mg L^{-1}) was added to the vials. For cotton stalk samples, three flasks of each treatment were harvested once a week and stored at −80 °C. All samples were lyophilized and weighed in 50 mL conical tubes. Then, 30 mL of MeOH was added to each tube. Samples were sonicated using an ultrasonic probe (20 kH), agitated for 30 min (200 rpm), and centrifuged (~4000 g, 15 min). Supernatants were filtered through a 0.2-μm Teflon filter and stored at −80 °C until analysis.

For quantitative analysis of CBZ, EP-CBZ, and *trans*-diOH-CBZ in the cotton stalk extracts, 250 μL of sample was diluted with 750 μL of ultrapure water, and an internal standard solution was added as described above. For qualitative analysis (identification of unknown metabolites), 3 mL of the extract

DOI: 10.1021/acs.est.5b02222
Environ. Sci. Technol. 2015, 49, 12351−12362

Table 1. Structures of Carbamazepine and Proposed Transformation Products Formed during Degradation by *P. ostreatus* during Solid-State Fermentation on Cotton Stalks

Name	Exact mass (Da)	Predicted formula	Structure	Primary substrate	Identification*
CBZ	237.1028	$C_{15}H_{12}N_2O$	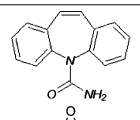		Standard
10,11-Epoxy carbamazepine (EP-CBZ)	253.0983	$C_{15}H_{12}N_2O_2$	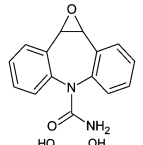	CBZ	Standard
***trans*-10,11-Dihydroxy carbamazepine (*trans*-diOH-CBZ)**	293.0910	$C_{15}H_{14}N_2O_3$	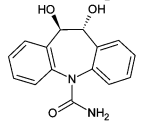	CBZ EP-CBZ	Standard
***cis*-10,11-Dihydroxy carbamazepine (*cis*-diOH-CBZ)**	293.0910	$C_{15}H_{14}N_2O_3$	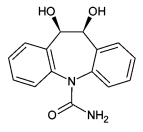	CBZ EP-CBZ	Standard
TP 251	251.0821	$C_{15}H_{10}N_2O_2$	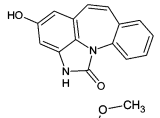	CBZ	Proposed
10-Methoxy-carbamazepine (10-methoxy-CBZ)	267.1132	$C_{16}H_{14}N_2O_2$	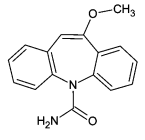	CBZ	Proposed
9-Acridine-caboxaldehyde	240.1025	$C_{15}H_{13}NO_2$	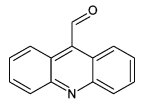	CBZ EP-CBZ Acridine	Proposed
Acridine	180.0815	$C_{13}H_9N$	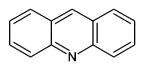	CBZ EP-CBZ Acridine	Standard
9-Hydroxy (9-OH) acridine	196.0764	$C_{13}H_9NO$	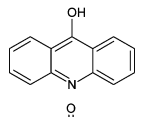	Acridine	Proposed
Acridone	196.0762	$C_{13}H_9NO$	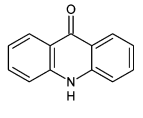	CBZ EP-CBZ Acridine	Standard
9-Acridine carboxylic acid	224.0712	$C_{14}H_9NO_2$	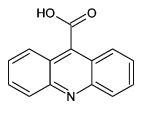	CBZ EP-CBZ Acridine	Standard
Hydroxyl (OH) 9-acridine carboxylic acid (four isomers)	240.0661	$C_{14}H_9NO_3$	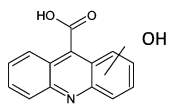	EP-CBZ Acridine	Proposed
TP 254	254.0821	$C_{15}H_{11}NO_3$	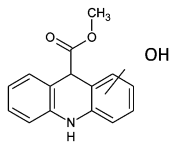	EP-CBZ Acridine	Proposed
TP 281	281.094	$C_{16}H_{12}N_2O_3$	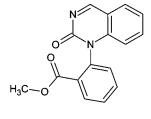	CBZ diOH-CBZ	Proposed

DOI: 10.1021/acs.est.5b02222
Environ. Sci. Technol. 2015, 49, 12351−12362

Table 1. continued

Name	Exact mass (Da)	Predicted formula	Structure	Primary substrate	Identification*
1-(2-Benzaldehyde)-(1H,3H)-quinazoline-2,4-one (BQD)	267.0771	$C_{15}H_{10}N_2O_3$	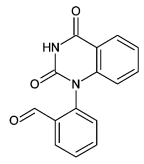	CBZ EP-CBZ diOH-CBZ	Proposed
TP 297	297.0875	$C_{16}H_{12}N_2O_4$	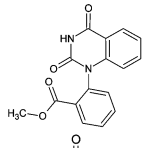	diOH-CBZ	Proposed
1-(2-Benzoic acid)-(1H,3H)-quinazoline-2,4-one (BaQD)	283.0725	$C_{15}H_{10}N_2O_4$	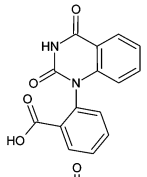	CBZ EP-CBZ diOH-CBZ	Ozone sample
TP 267	267.0771	$C_{15}H_{10}N_2O_3$	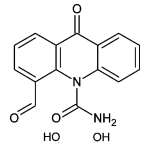	CBZ diOH-CBZ	Proposed
TP 272	272.0932	$C_{15}H_{13}NO_4$	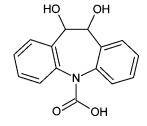	CBZ diOH-CBZ	Proposed
TP 286	286.1085	$C_{16}H_{15}NO_4$	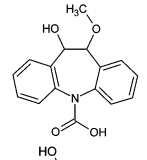	CBZ EP-CBZ diOH-CBZ	Proposed
10-Hydroxy carbamazepine (10-OH CBZ)	255.1124	$C_{15}H_{14}N_2O_2$	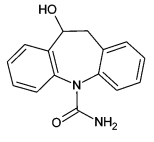	diOH-CBZ	Proposed
TP 208	208.0760 (neg: 224.071)	$C_{14}H_9NO$ $C_{14}H_{11}NO_2$	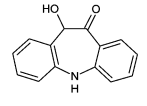	CBZ diOH-CBZ	Proposed

*TPs were identified as (1) "Standard" (identified by comparison of retention time and product ion spectra with synthesized compounds), (2) "Proposed" (tentative assignments based on interpretation of product ion spectra), or (3) "Ozone sample" (on the basis of comparison with CBZ ozone treatment).[26]

was dried under a gentle N_2 stream, reconstituted in 400 μL of MeOH, and vortexed rigorously. Then, 100 μL of sample was mixed with 100 μL of ultrapure water and centrifuged (10 000 g, 10 min). The supernatant was moved to a clean vial prior to LC−MS analysis.

Analytical Procedures. Quantification of CBZ, EP-CBZ, and *trans*-diOH-CBZ used as primary substrates was conducted by LC−MS using the Agilent 1200 Rapid Resolution LC system (Agilent Technologies Inc., Santa Clara, CA) and an Acclaim C18 RSLC column (Dionex, Sunnyvale, CA; 2.1 × 150 mm^2, particle size 2.2 μm). Separation conditions are detailed in Table S1. The LC system was coupled with an Agilent 6410 triple quad mass selective detector equipped with an electrospray ionization ion source. The mass spectrometer was operated in positive ionization mode. Ion source parameters were as follows: capillary voltage, 4000 V; drying gas (nitrogen, 99%) temperature and flow, 350 °C and 10 L min^{-1}, respectively; nebulizer pressure, 35 psi; and nitrogen (99.999%) collision gas. The LC−MS system was controlled and data were analyzed using MassHunter software (Agilent Technologies Inc.). Quantitative analysis was performed in multiple reaction monitoring (MRM) mode with isotopically labeled analogues as internal standards, and the MRM parameters are listed in Table S2.

Qualitative analysis of additional TPs formed during solid-state fermentation on cotton stalks was performed on a Waters ACQUITY UPLC system connected to a Synapt G2S equipped with an electrospray ionization source (Waters Corp., Milford, CT, USA). Negative and positive modes were used to elucidate the compounds by MarkerLynx and UniFi, as described by Seiwert et al.[31] Peak areas were calculated by TargetLynx to produce a temporal trend for each TP. In Table 1, TPs were identified as (1) "standard" (by comparison of retention time and product ion spectra with synthesized compounds), (2) "proposed" (i.e., tentative assignments on the basis of interpretation of product ion spectra), or (3) "ozone sample"

DOI: 10.1021/acs.est.5b02222
Environ. Sci. Technol. 2015, 49, 12351−12362

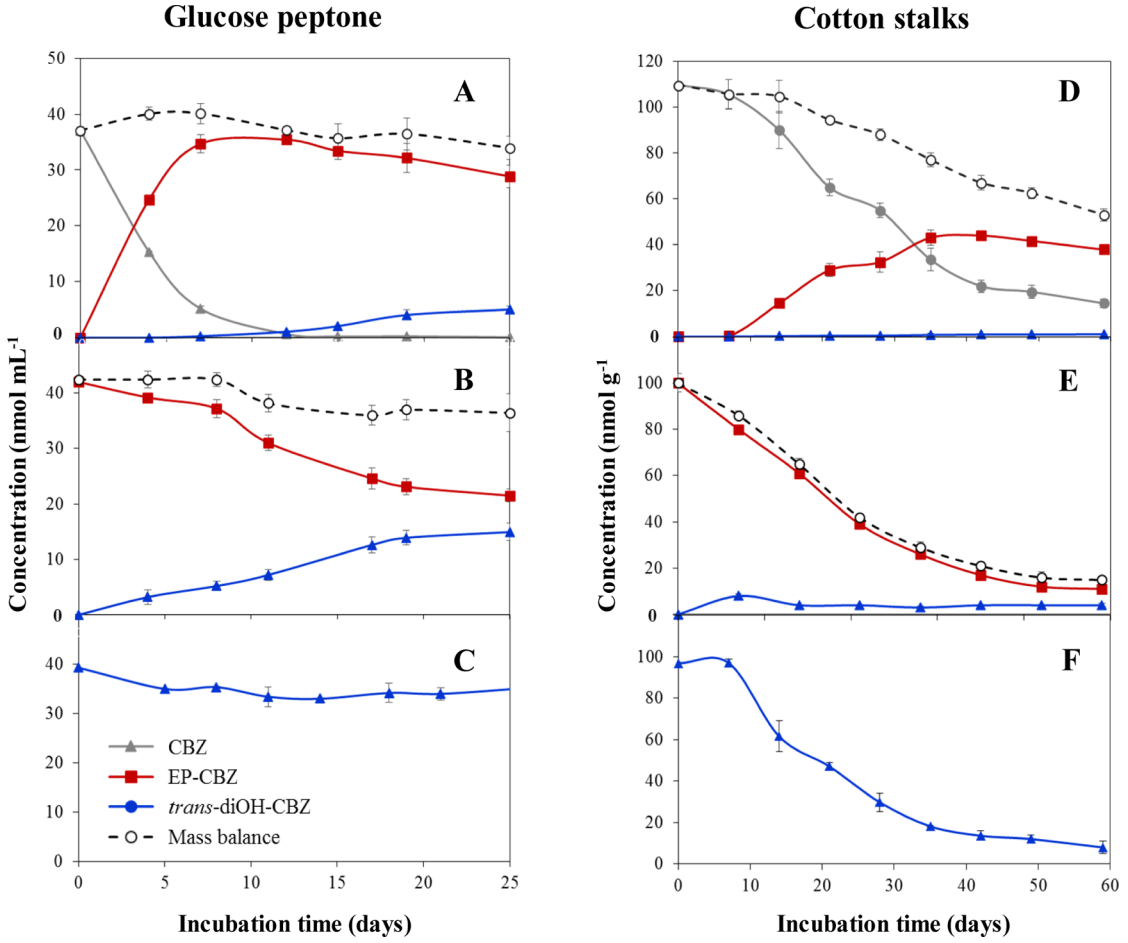

Figure 1. Dissipation of the primary substrates carbamazepine (CBZ; A and D), 10,11-epoxy carbamazepine (EP-CBZ; B and E), and *trans*-10,11-dihydroxy carbamazepine (*trans*-diOH-CBZ; C and F) by *P. ostreatus* in GP medium (left) and during solid-state fermentation on cotton stalks (right). Plotted values are means ± SD of three replicates. Mass-balance data are presented by dashed lines and open sympols.

(on the basis of comparison with CBZ ozone treatment).[26] Identification of TP 251, *cis*-diOH-CBZ, 10-methoxy-CBZ, 9-acridine carboxylic acid, acridine, acridone, 9-acridine carboxaldehyde, 1-(2-benzaldehyde)-(1H,3H)-quinazoline-2,4-dione (BQD), 1-(2-benzoicacid)-(1H,3H)-quinazoline-2,4-dione (BaQD), TP 267, TP 286, TP 281, and TP 272 was based on a comparison with data generated by electrochemical oxidation as detailed elsewhere.[31] Distinguishing between cis and trans isomers was according to retention time (3.80 and 5.47 min, respectively). Identification of 9-OH acridine, OH-9-acridine carboxylic acid (a–d), 10-OH-CBZ, TP 297, TP 254, and TP 208 (Table 1) is detailed in the Table S3.

RESULTS AND DISCUSSION

Degradation of CBZ: Substrate Effects. When *P. ostreatus* was cultivated in liquid GP medium, 99% dissipation of CBZ was observed (Figure 1A). After 7 days, CBZ was transformed to EP-CBZ (78%) and diOH-CBZ (13.5%), which were the only metabolites formed under these conditions. Because no other TPs were identified in this experimental setup, we suggest that about 10% of the added CBZ was sorbed to the fungal biomass, as observed previously.[7,17] When EP-CBZ was applied as the primary substrate (Figure 1B), ∼50% of it dissipated, ∼35% was transformed to diOH-CBZ, and the mass balance was 87%. This may suggest that either EP-CBZ is transformed by additional pathways or its degradation rate is slower than that of diOH-CBZ. Both assumptions were ruled out because no other metabolites were identified in this system. As suggested for CBZ, it is likely that 13% of the added EP-CBZ was sorbed to the fungal biomass. When diOH-CBZ was introduced as the primary substrate (Figure 1C), its level was stable, and no TPs were detected. It was concluded that in rich liquid medium, *P. ostreatus* cannot metabolize diOH-CBZ, making it a dead-end product. In uninoculated GP medium controls, concentrations of CBZ, EP-CBZ, and diOH-CBZ were constant during the entire incubation period, demonstrating that in the inoculated cultures removal of CBZ and EP-CBZ was biological and occurred solely by *P. ostreatus*.

Our hypothesis was that during solid-state fermentation using natural lignocellulosic substrate (i.e., cotton stalks) *P. ostreatus* physiology and its enzymatic profile would be tuned toward lignin degradation.[22,23] This might affect the transformation pathway and lead to the formation of additional metabolites. Indeed, when CBZ was introduced as the primary substrate on cotton stalks, major differences in its fate as compared to that in liquid medium were observed (Figure 1D). EP-CBZ accumulated to a lower level, and diOH-CBZ comprised less than 1% of the initial CBZ amount. Furthermore, in contrast to the liquid medium, mass-balance analysis revealed that the sum of CBZ and it TPs decreases during the incubation period constituting only 50% of the initial CBZ amount after 60 days of incubation (Figure 1D).

DOI: 10.1021/acs.est.5b02222
Environ. Sci. Technol. 2015, 49, 12351−12362

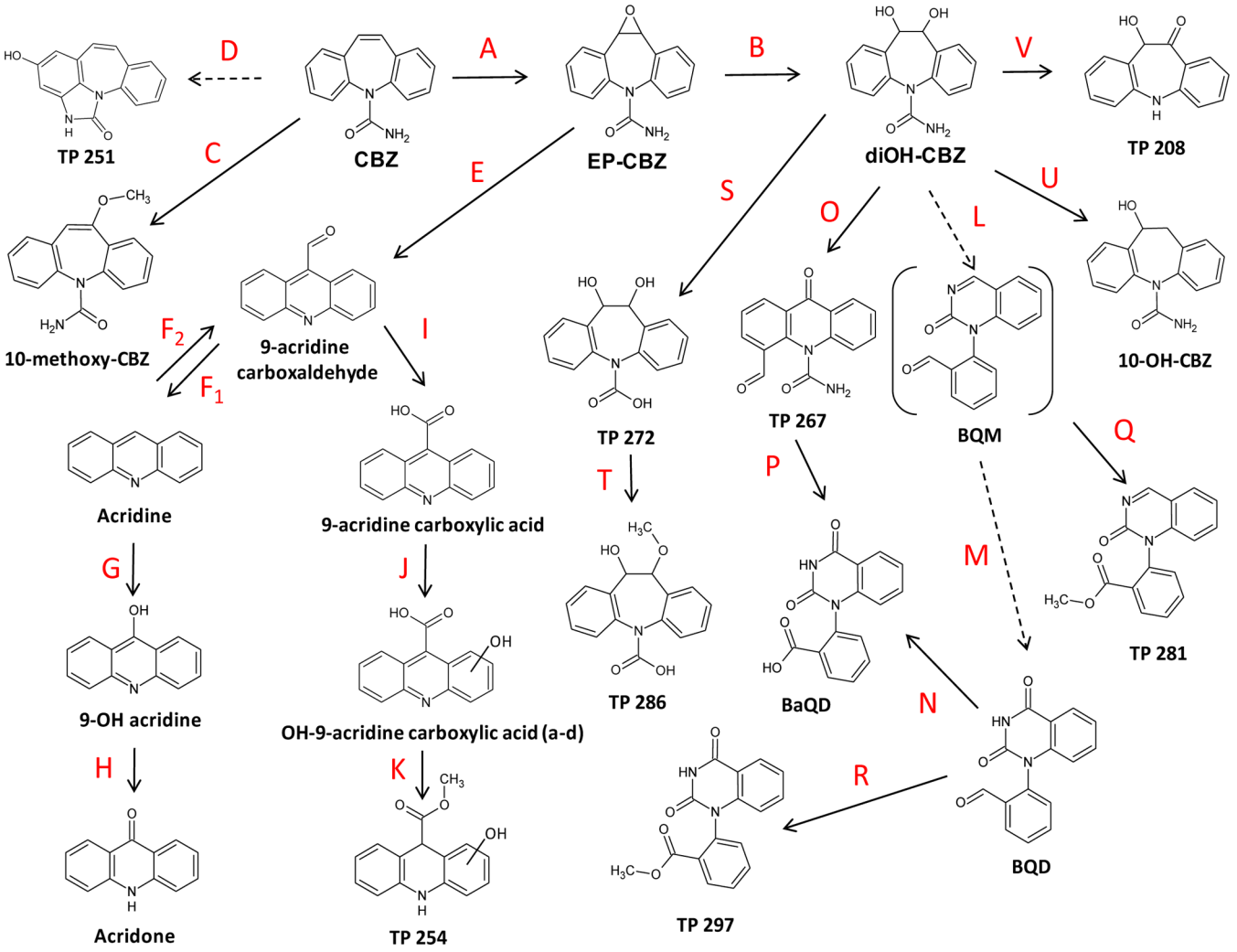

Figure 2. Proposed pathways for CBZ metabolism by *P. ostreatus* during solid-state fermentation on cotton stalks. Transformation products are marked with numbers as detailed in Table 1; reactions are marked with letters (A–V).

Differences between the two media were also observed when EP-CBZ was used as the primary substrate (Figure 1E): 90% of the added EP-CBZ dissipated, and diOH-CBZ did not accumulate. This suggested that other degradation products besides diOH-CBZ had been formed. Under solid-state conditions, diOH-CBZ as the primary substrate exhibited significant dissipation (Figure 1F). These results suggest that under these conditions the complex enzymatic systems produced by the fungus are capable of further transforming this metabolite unlike the dead-end scenario observed for the GP medium. In uninoculated cotton stalk controls, concentrations of CBZ, EP-CBZ and diOH-CBZ were constant throughout the incubation period.

Proposed Pathway for Transformation of CBZ during Solid-State Fermentation. A total of 24 TPs were tentatively identified when CBZ was metabolized by *P. ostreatus* during solid-state fermentation (Table 1 and Figure 2). A combination of electrochemical oxidation and LC–HRMS proved to be very useful in detecting and identifying many of these TPs.[31] To better understand the transformation pathways, the main CBZ metabolites were used separately as primary substrates, and the TPs were analyzed at several time points during incubation. This approach enabled us to cluster the TPs into the proposed subpathways and to detect TPs that were below detection levels when CBZ was the primary substrate.

CBZ transformation by *P. ostreatus* during solid-state fermentation on cotton stalks could be divided into three subpathways. The main pathway was oxidation of CBZ to the reactive and pharmacologically active EP-CBZ[32] (Figure 2, reaction A), by either cytochrome P-450 or manganese peroxidase or both, as has been shown to occur in liquid culture.[17] Then, further hydrolysis of EP-CBZ to diOH-CBZ occurred (Figure 2, reaction B). This reaction is known to be catalyzed by epoxide hydrolase in human and rat liver.[33] Because epoxide hydrolase genes are found in the *P. ostreatus* genome (JGI genome database of *P. ostreatus* PC9 v1.0),[34] we suggest that these gene products catalyze the hydrolysis of EP-CBZ in *P. ostreatus* as well. EP-CBZ was also metabolized via the acridine pathway (Figure 2, reactions E–K), and diOH-CBZ was further transformed to a variety of compounds (Figure 2, reactions L–V). CBZ was metabolized via two additional pathways (Figure 2, reactions C and D): Reaction C (methoxylation of CBZ) formed 10-methoxy-CBZ. Methoxylation and methylation reactions are well-known to occur during lignin degradation by white-rot fungi, along with demethoxylation and demethylation.[1,2] Similar reactions are active during the degradation of chlorinated aromatic

DOI: 10.1021/acs.est.5b02222
Environ. Sci. Technol. 2015, 49, 12351–12362

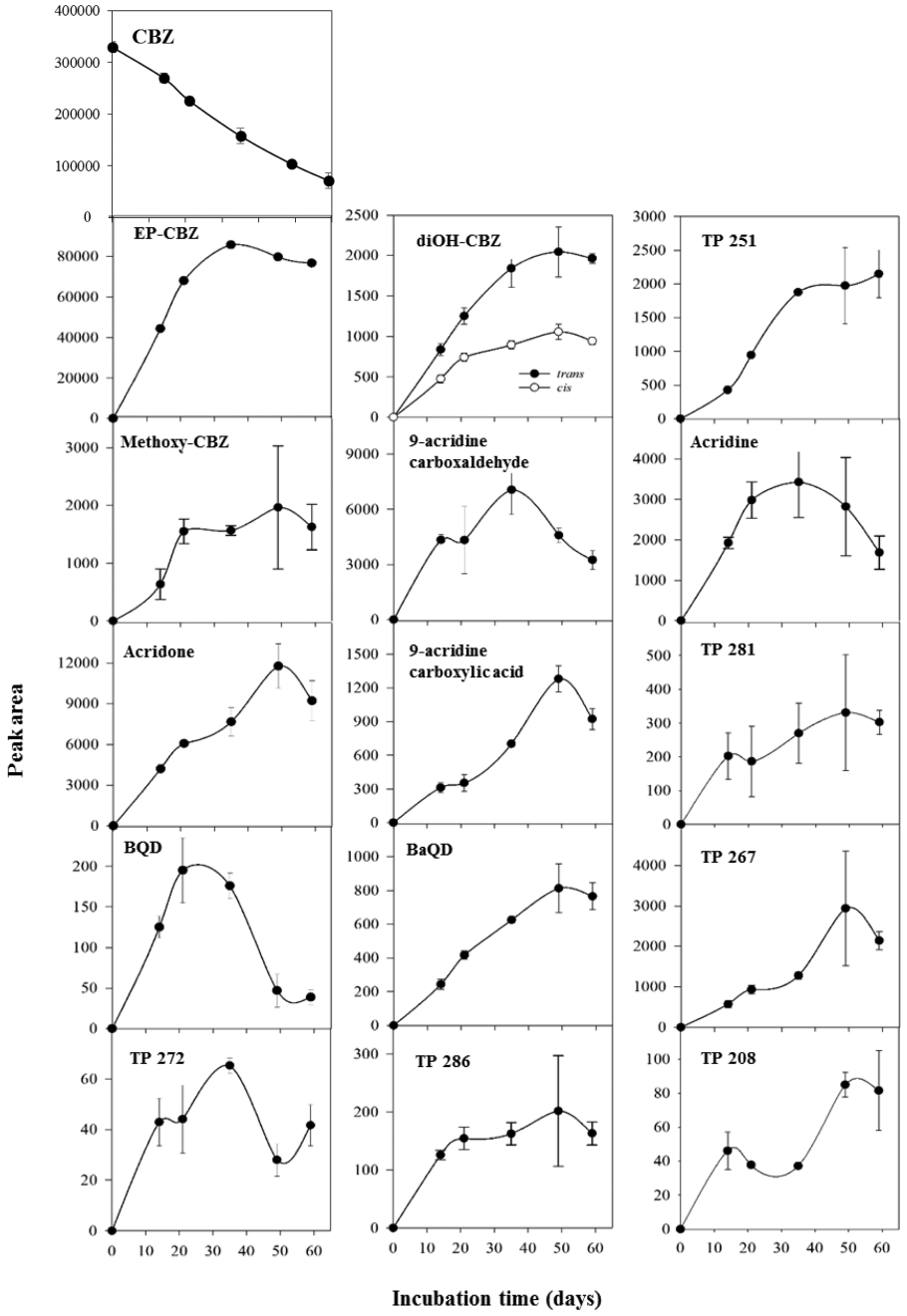

Figure 3. Peak area trends of carbamazepine as primary substrate and transformation products identified during its dissipation by *P. ostreatus* grown on cotton stalks. Plotted values are means ± SD of three replicates.

compounds by *Phanerochaete chrysosporium*.[35] However, it was suspected that methylation might be due to the use of methanol in the extraction. Upon repeated extraction with acetonitrile, TP 286 was still observed, showing that *P. ostreatus* was indeed able to methylate the TPs. The peak area of 10-methoxy-CBZ showed a decreasing trend, which might indicate further transformation or demethoxylation redirecting the reaction toward the parent compound. Reaction D (Figure 2) led to the formation of TP 251 (proposed structure; Table 1 and Figure 2). This compound can be formed via monohydroxylation of CBZ to 2-OH-CBZ and subsequent formation of iminoquinone, followed by internal cyclization of the carbamoyl group with the carbon in position 6. However, these intermediate products were not detected in any of the samples. This might be due to their rapid transformation to TP 251. Transformation of CBZ to 2-OH-CBZ and formation of the reactive metabolite iminoquinone have been shown to occur in the human liver.[36] TP 251 seems to be quite stable because its peak area showed an increasing trend during the incubation period (Figure 3).

Two subpathways were derived from EP-CBZ, one leading to both *cis*- and *trans*-diOH-CBZ (Figure 2, reaction B), and the second leading to a variety of acridine-like TPs (Figure 2, reaction E). Formation of the uncommon isomer *cis*-diOH-CBZ (Table 1) seemed to be minor because its peak area was smaller than that of *trans*-diOH-CBZ (Figures 3 and 4). Both diOH-CBZ isomers were detected when EP-CBZ was applied as the primary substrate, and they showed a similar increasing trend followed by a slight decrease at the end of the incubation

DOI: 10.1021/acs.est.5b02222
Environ. Sci. Technol. 2015, 49, 12351−12362

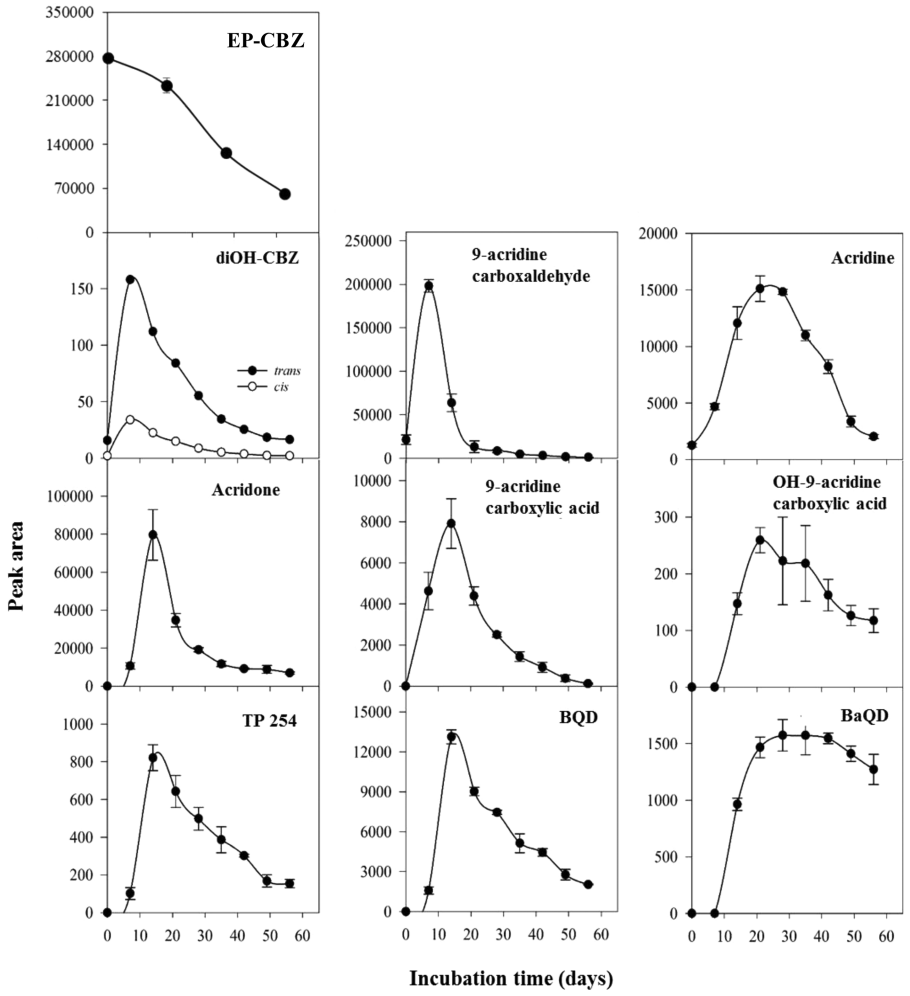

Figure 4. Peak area trends of 10,11-epoxy carbamazepine as primary substrate and transformation products identified during its dissipation by *P. ostreatus* grown on cotton stalks. Plotted values are means ± SD of three replicates.

(Figure 4). To the best of our knowledge, there is no evidence for biological *cis*-hydrolysis of EP-CBZ.

Reaction E (Figure 2) led to the formation of 9-acridine-carboxaldehyde (Table 1), which is known to be toxic and reactive. This compound is formed from EP-CBZ by loss of the carbamoyl moiety accompanied by a contraction of the seven-membered ring of EP-CBZ into a six-membered ring.[37] Indeed, when ^{14}C-carbonyl-labeled CBZ was used as the substrate, ^{14}C-CO_2 release amounted to 17.4% of the initial radioactivity after 63 days of incubation. ^{14}C-CO_2 formation rate was maximal during the third week of incubation; then a slow, yet constant, ^{14}C-CO_2 release was observed until the end of the experiment (Figure S2). These may represent different reactions in the transformation pathway (e.g., reaction E and V, Figure 2). Incubation of ^{14}C -CBZ in soil resulted in mineralization of only 1% of ^{14}C-CO_2 released after 120 days, demonstrating its extreme stability in natural environments.[38] Reaction E (Figure 2) has been shown to occur in the peripheral blood of patients treated with CBZ.[39] Direct formation of 9-acridine-carboxaldehyde from CBZ has also been shown to occur in activated leukocytes under strong oxidative conditions.[40] However, in the current study, its peak area reached a maximum during the first week of incubation with EP-CBZ as the substrate but only after 5 weeks with CBZ as the substrate (Figures 4 and 3, respectively). This supports our hypothesis that under solid-state fermentation conditions 9-acridine-carboxaldehyde is formed from EP-CBZ rather than directly from CBZ. This difference in the timing of formation of a certain TP in emphasizes the advantages of using metabolites as primary substrates for elucidating pathways. 9-Acridine-carboxaldehyde is highly reactive and has been previously reported to bind covalently to neutrophils.[40] The next reaction was cleavage of the aldehyde moiety of 9-acridine-carboxaldehyde, leading to acridine formation (Figure 2, reaction F_1). This was concluded by the time profile of acridine formation in both the CBZ and EP-CBZ experiments (Figures 3 and 4, respectively). Interestingly, 9-acridine-carboxaldehyde was also detected in samples in which acridine has been added as the primary substrate, meaning that the opposite reaction is also possible under these conditions (i.e., acridine can undergo addition of an aldehyde group; Figure 2, reaction F_2). This reaction has never been reported in either biological or chemical systems.

Acridine was further oxidized to 9-OH acridine (Figure 2, reaction G), which was subsequently transformed to acridone (Figure 2, reaction H). To verify this pathway, we also applied acridine as a primary substrate (Figure S3) and found the presence of 9-OH acridine to increase first, followed by that of acridone, indicating that 9-OH acridine is an intermediate between acridine and acridone (Figure S3). Acridine is toxic to both aquatic and terrestrial organisms,[41,42] and its oxidation to

DOI: 10.1021/acs.est.5b02222
Environ. Sci. Technol. 2015, 49, 12351−12362

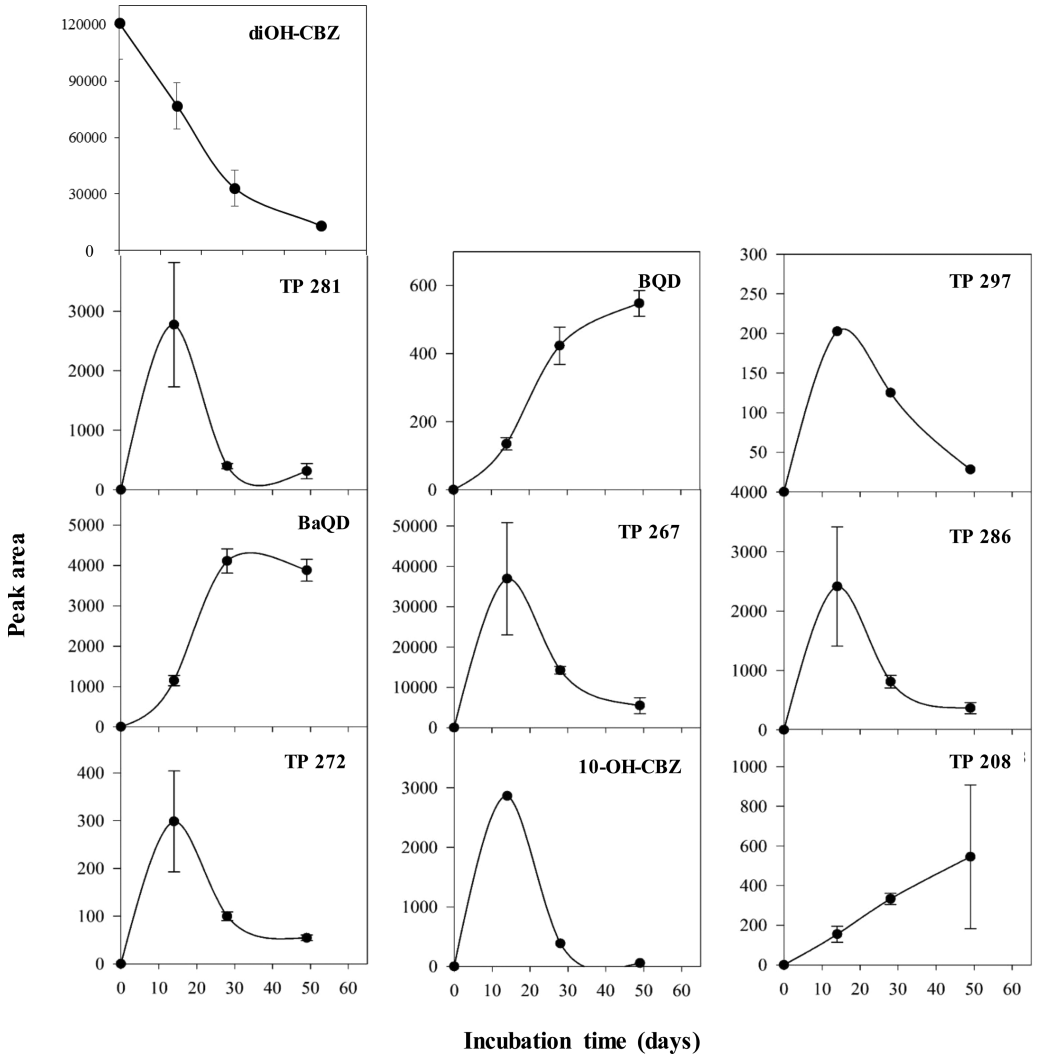

Figure 5. Peak area trends of *trans*-10,11-dihydroxy carbamazepine as primary substrate and transformation products identified during its dissipation by *P. ostreatus* grown on cotton stalks. Plotted values are means ± SD of three replicates.

acridone is a well-known biological detoxification process, the latter being considered nontoxic.[39] This oxidation occurs by the enzyme aldehyde oxidase in rat liver cells as well as in mussel and other aquatic invertebrates.[43] Genes encoding such enzymes have been found in the *P. ostreatus* genome (JGI genome database of *P. ostreatus* PC9 v1.0).[34] In both treatments, when EP-CBZ and acridine were used as the primary substrates, the acridone peak area showed a decreasing trend after 2 weeks of incubation, indicating that it is subsequently transformed (Figures 4 and S1). However, we were not able to detect any downstream TPs. This is in agreement with the fact that in a previous report no further TPs were detected during acridone removal in biological systems.[27] An additional subpathway derived from 9-acridine-carboxaldehyde was oxidation, forming the toxic and reactive 9-acridine carboxylic acid (Figure 2, reaction I). This reaction has been shown to occur during activated sludge treatment.[27]

Subsequent hydroxylation of 9-acridine carboxylic acid formed all four possible isomers of OH-9-acridine carboxylic acid (Figure 2, reaction J), with the peak areas of all showing a moderate decrease starting from day 21 (Figures 4 and S3). Formation of OH-9-acridine carboxylic acid has been reported during activated sludge treatment and in contact with sand filter material;[27] however, in none of those treatments were all four isomers detected. In both treatments in which EP-CBZ and acridine were applied as a primary substrate, a methylated form of OH-9-acridine carboxylic acid (TP 254) was detected (Figure 2, reaction K), also showing a decreasing trend and suggesting possible further transformation or demethylation back to OH-9-acridine carboxylic acid.

The proposed pathway of *trans*-diOH-CBZ transformation by *P. ostreatus* under solid-state fermentation conditions could be divided into five subpathways (Figure 2, reactions L, O, S, U, and V). The pathway leading to BQM, BQD, and BaQD (Figure 2, reactions L–N) has been discussed extensively during ozonation of CBZ[26,28] and upon UV irradiation of EP-CBZ.[44] In the case of CBZ, ozone attacks and cleaves the 10–11 bond, forming 1-(2-benzaldehyde)-4-hydro-(1H,3H)-quinazoline-2-one (BQM), which is subsequently oxidized to BQD that is then oxidized by OH radicals to BaQD. During lignin degradation by white-rot fungi, free radicals are formed, and the conditions are highly oxidative.[2] Thus, we suggest that the mechanism of the BQD pathway in *P. ostreatus* is similar with a few modifications. First, because TPs of the BQD pathway were all detected in the *trans*-diOH-CBZ treatment, we conclude that under these conditions BQD is not formed directly from

DOI: 10.1021/acs.est.5b02222
Environ. Sci. Technol. 2015, 49, 12351–12362

CBZ or EP-CBZ but rather only from *trans*-diOH-CBZ. Second, BQM was identified only as a methoxylated derivative (TP 281, Table 1); thus, we suggest that BQM was formed from *trans*-diOH-CBZ and then oxidized to BQD (Figure 2, reaction M). BQM methoxylation to TP 281 (Figure 2, reaction Q) can occur either in vivo, in parallel to its oxidation, or during the extraction procedure with methanol, as already noted. In samples in which CBZ was the primary substrate, the peak area of TP 281 showed an increasing trend with a slight decrease at the end of the incubation (Figure 3). However, in samples with *trans*-diOH-CBZ as the primary substrate, it decreased rapidly, suggesting a further transformation (Figure 5), possibly oxidation to TP 297 (methoxylated BQD; reaction R, Figure 2). The peak area of BQD showed a decreasing trend after 14−21 days of incubation with CBZ and EP-CBZ (Figures 3 and 4, respectively), indicating its further oxidation to BaQD (Figure 2, reaction N). However, in *trans*-diOH-CBZ samples, it showed a moderate increase throughout the entire incubation period (Figure 5). This might be explained by a rapid formation rate when *trans*-diOH-CBZ is the primary substrate (vs CBZ and EP-CBZ), which may lead to its accumulation.

Similar to BQM, BQD can be methoxylated to TP 297 either in vivo or during the extraction procedure. BaQD showed an increasing trend in all treatments (Figures 3−5), followed by a slight decrease, most prominently with EP-CBZ as primary substrate (Figure 4). This suggests further, albeit very slow transformation. BaQD formed during ozonation has been shown to be resistant to microbial degradation in a sand filter.[26] An additional pathway leading to BaQD was from *trans*-diOH-CBZ via TP 267 (Figure 2, reactions O and P). The latter formed from *trans*-diOH-CBZ by 10−11 bond cleavage followed by intramolecular ring closure and dehydration (Figure 2, reaction O); TP 267 then underwent an internal rearrangement followed by oxidation, forming BaQD (Figure 2, reaction P). This is compatible with the decreasing peak area of TP 267 at longer incubation times (Figures 3 and 5). Formation of BaQD from TP 267 is also supported by the CBZ transformation observed during electrochemical oxidation.[31]

Reaction S (Figure 2) was hydrolysis of the carbamoyl moiety of *trans*-diOH-CBZ to a carboxylic acid group, forming TP 272. To the best of our knowledge, this reaction has never been reported. A proposed mechanism might be similar to that of the transformation of atenolol to atenolol acid by amidohydrolase produced by bacteria (EAWAG biocatalysis/biotransformation database).[45] The methylated form of TP 272 (TP 286) was identified in both CBZ and *trans*-diOH-CBZ samples (Figure 2, reaction T).

Reaction U (Figure 2) led to the formation of 10-OH-CBZ, which was the only product unique to the *trans*-diOH-CBZ treatment and was not detected in the control sample. Its peak area showed a decreasing trend (Figure 5) after 2 weeks, suggesting subsequent transformation.

The fifth pathway (Figure 2, reaction V) led to TP 208, formed by dehydrogenation of *trans*-diOH-CBZ followed by elimination of the carbamoyl group. This compound has been reported to form from CBZ during oxidation by ferrate via electrophilic attack on the 10−11 double bond. CBZ-ketol is then formed by electron transfer from CBZ to the oxidant, accompanied by hydrolysis of the carbamoyl group.[25] Formation of CBZ-ketol has also been described to occur during activated sludge treatment via dehydrogenation of *trans*-diOH-CBZ. However, TP 208 was not identified in the latter study but rater was proposed as an intermediate to the formation of 9-acridine carboxaldehyde. Nevertheless, this was not the case in the current study because we identified 9-acridine carboxaldehyde only in samples treated with EP-CBZ. Moreover, the peak area of TP 208 showed an increasing trend throughout the entire incubation period in both CBZ (Figure 3) and *trans*-diOH-CBZ (Figure 5) treatments, meaning that under these conditions it is not further transformed.

This work highlights the effect of growth conditions on the biotransformation pathways of xenobiotics. Under certain conditions, a wide array of TPs can form. Hence, using the major metabolites as primary substrates can be a rational and feasible approach to elucidate the transformation pathways.

■ ENVIRONMENTAL IMPLICATIONS

The widely used anticonvulsant pharmaceutical CBZ exhibits limited removal efficiency during conventional wastewater treatment and is recalcitrant to degradation by natural soil microorganisms.[46,47] CBZ has been shown to be taken up by crops irrigated with reclaimed wastewater[48,49] and may negatively affect both humans and the ecosystem.[50−53] Thus, this xenobiotic is targeted for advanced chemical and physical treatments.[16,24−28] In this paper, we described an alternative, environmentally friendly, biological treatment for CBZ degradation. Environmentally relevant CBZ concentrations were applied using our solid-state fermentation. CBZ was introduced at concentration of 25 $\mu g\ g^{-1}$ cotton stalks, whereas in biosolids, CBZ concentration was reported in a range of 3.4−258 $\mu g\ kg^{-1}$.[54] The higher concentrations used in some of the experiments enable us to detect and identify TPs. In addition, the elimination rate of CBZ was similar in both liquid and solid-state mediums at much lower concentrations (1 and 0.025 $\mu g\ g^{-1}$, respectively),[17] as noted in Figure S4. In this case, the applied CBZ concentration is even relevant for its concentration in reclaimed wastewater.[55,56]

The transformation efficiency of CBZ has been shown to be dependent on environmental conditions, leading to different metabolic pathways involving different TPs. Growing the fungus *P. ostreatus* under solid-state-fermentation conditions on lignocellulosic substrate in the presence of CBZ enabled the latter's further degradation, probably because of the activity of the ligninolytic system. The degradation of many other aromatic pollutants, such as polycyclic aromatic hydrocarbons, polychlorinated biphenyls, dyes, and explosives, has been attributed to lignin-degrading enzymes.[4] Another white-rot fungus, *T. versicolor*, was able to degrade pharmaceutical compounds in nonsterile sewage sludge[57] and in a fluidized-bed bioreactor fed with nonsterile urban wastewater.[6] The potential and limitations of using wood-decay fungi for bioremediation have been discussed over the years.[57,58] Combining these data with those described here suggest the practical application of white-rot fungi as a valid option for the treatment of pollutants. However, before applying a new treatment method, it is important to thoroughly understand the transformation pathways occurring under different environmental conditions to ensure that new hazardous are not produced and new potential risks are not evolved.

■ ASSOCIATED CONTENT

Supporting Information

The Supporting Information is available free of charge on the ACS Publications website at DOI: 10.1021/acs.est.5b02222.

DOI: 10.1021/acs.est.5b02222
Environ. Sci. Technol. 2015, 49, 12351−12362

HPLC conditions used to separate CBZ, EP-CBZ, and diOH-CBZ (Table S1), the MRM parameters for quantification of CBZ, EP-CBZ, and diOH-CBZ (Table S2), identification of TPs formed during solid-state fermentation (Table S3), ^{14}C-CBZ labeling (Figure S1), the accumulation of ^{14}C-CO_2 formed during degradation of ^{14}C-CBZ by *P. ostreatus* in solid-state fermentation on cotton stalks (Figure S2), peak area trends of TPs identified during the dissipation of acridine (Figure S3), and removal of CBZ at an environmentally relevant concentration during growth on cotton stalks (Figure S4).(PDF)

AUTHOR INFORMATION

Corresponding Author

*Tel.: (+972) 8-948-9935. Fax: (+972) 8-946-8785. E-mail: yitzhak.hadar@mail.huji.ac.il.

Notes

The authors declare no competing financial interest.

ACKNOWLEDGMENTS

This study was partially supported by grants from DFG (project Re1290/7-1, PECtake), the United States−Israel Binational Agricultural Research and Development Fund (BARD, US-4551-12), and the Israeli Ministry of Agriculture. N.G.-R. is the recipient of a partial Ph.D. fellowship from the Israel Water Authority. We thank Prof. Oded Yarden for useful comments throughout the project and Prof. Baruch Rubin and his lab members for the advice and hospitality in the radioactive-certified facility.

REFERENCES

(1) Higuchi, T. Lignin biochemistry - biosynthesis and biodegradation. *Wood Sci. Technol.* **1990**, *24* (1), 23−63.

(2) Kirk, T. K.; Farrell, R. L. Enzymatic "combustion": The microbial degradation of lignin. *Annu. Rev. Microbiol.* **1987**, *41*, 465−505.

(3) Hofrichter, M.; Ullrich, R.; Pecyna, M. J.; Liers, C.; Lundell, T. New and classic families of secreted fungal heme peroxidases. *Appl. Microbiol. Biotechnol.* **2010**, *87* (3), 871−897.

(4) Hadar, Y.; Cullen, D., Organopollutant degradation by wood decay basidiomycetes. In *The Mycota, Agricultural Applications*, 2 ed.; Kempken, F.E., Ed.; Springer-Verlag: Berlin, 2013; Vol. *11*.

(5) Badia-Fabregat, M.; Rosell, M.; Caminal, G.; Vicent, T.; Marco-Urrea, E. Use of stable isotope probing to assess the fate of emerging contaminants degraded by white-rot fungus. *Chemosphere* **2014**, *103*, 336−342.

(6) Cruz-Morato, C.; Ferrando-Climent, L.; Rodriguez-Mozaz, S.; Barcelo, D.; Marco-Urrea, E.; Vicent, T.; Sarra, M. Degradation of pharmaceuticals in non-sterile urban wastewater by *Trametes versicolor* in a fluidized bed bioreactor. *Water Res.* **2013**, *47* (14), 5200−5210.

(7) Marco-Urrea, E.; Perez-Trujillo, M.; Vicent, T.; Caminal, G. Ability of white-rot fungi to remove selected pharmaceuticals and identification of degradation products of ibuprofen by *Trametes versicolor*. *Chemosphere* **2009**, *74* (6), 765−772.

(8) Rodarte-Morales, A. I.; Feijoo, G.; Moreira, M. T.; Lema, J. M. Degradation of selected pharmaceutical and personal care products (PPCPs) by white-rot fungi. *World J. Microbiol. Biotechnol.* **2011**, *27* (8), 1839−1846.

(9) Rodarte-Morales, A. I.; Feijoo, G.; Moreira, M. T.; Lema, J. M. Operation of stirred tank reactors (STRs) and fixed-bed reactors (FBRs) with free and immobilized *Phanerochaete chrysosporium* for the continuous removal of pharmaceutical compounds. *Biochem. Eng. J.* **2012**, *66*, 38−45.

(10) Rodriguez-Rodriguez, C. E.; Marco-Urrea, E.; Caminal, G. Degradation of naproxen and carbamazepine in spiked sludge by slurry and solid-phase *Trametes versicolor* systems. *Bioresour. Technol.* **2010**, *101* (7), 2259−2266.

(11) Kang, S. I.; Kang, S. Y.; Hur, H. G. Identification of fungal metabolites of anticonvulsant drug carbamazepine. *Appl. Microbiol. Biotechnol.* **2008**, *79* (4), 663−669.

(12) Marco-Urrea, E.; Radjenovic, J.; Caminal, G.; Petrovic, M.; Vicent, T.; Barcelo, D. Oxidation of atenolol, propranolol, carbamazepine and clofibric acid by a biological Fenton-like system mediated by the white-rot fungus *Trametes versicolor*. *Water Res.* **2010**, *44* (2), 521−532.

(13) Jelic, A.; Cruz-Morato, C.; Marco-Urrea, E.; Sarra, M.; Perez, S.; Vicent, T.; Petrovic, M.; Barcelo, D. Degradation of carbamazepine by *Trametes versicolor* in an air pulsed fluidized bed bioreactor and identification of intermediates. *Water Res.* **2012**, *46* (4), 955−964.

(14) Ba, S.; Jones, J. P.; Cabana, H. Hybrid bioreactor (HBR) of hollow fiber microfilter membrane and cross-linked laccase aggregates eliminate aromatic pharmaceuticals in wastewaters. *J. Hazard. Mater.* **2014**, *280*, 662−670.

(15) Nguyen, L. N.; Hai, F. I.; Price, W. E.; Leusch, F. D. L.; Roddick, F.; Ngo, H. H.; Guo, W.; Magram, S. F.; Nghiem, L. D. The effects of mediator and granular activated carbon addition on degradation of trace organic contaminants by an enzymatic membrane reactor. *Bioresour. Technol.* **2014**, *167*, 169−177.

(16) Touahar, I. E.; Haroune, I.; Ba, S.; Bellenger, J.-P.; Cabana, H. Characterization of combined cross-linked enzyme aggregates from laccase, versatile peroxidase and glucose oxidase, and their utilization for the elimination of pharmaceuticals. *Sci. Total Environ.* **2014**, *481*, 90−99.

(17) Golan-Rozen, N.; Chefetz, B.; Ben-Ari, J.; Geva, J.; Hadar, Y. Transformation of the recalcitrant pharmaceutical compound carbamazepine by *Pleurotus ostreatus*: role of cytochrome P450 monooxygenase and manganese peroxidase. *Environ. Sci. Technol.* **2011**, *45* (16), 6800−6805.

(18) Wariishi, H.; Valli, K.; Gold, M. H. *In-vitro* depolymerization of lignin by manganese peroxidase of *Phanerochaete chrysosporium*. *Biochem. Biophys. Res. Commun.* **1991**, *176* (1), 269−275.

(19) Knop, D.; Ben-Ari, J.; Salame, T. M.; Levinson, D.; Yarden, O.; Hadar, Y. Mn^{2+}-deficiency reveals a key role for the *Pleurotus ostreatus* versatile peroxidase (VP4) in oxidation of aromatic compounds. *Appl. Microbiol. Biotechnol.* **2014**, *98* (15), 6795−6804.

(20) Knop, D.; Yarden, O.; Hadar, Y. The ligninolytic peroxidases in the genus *Pleurotus*: divergence in activities, expression, and potential applications. *Appl. Microbiol. Biotechnol.* **2015**, *99*, 1025−1038.

(21) Giardina, P.; Faraco, V.; Pezzella, C.; Piscitelli, A.; Vanhulle, S.; Sannia, G. Laccases: a never-ending story. *Cell. Mol. Life Sci.* **2010**, *67* (3), 369−385.

(22) Pezzella, C.; Lettera, V.; Piscitelli, A.; Giardina, P.; Sannia, G. Transcriptional analysis of *Pleurotus ostreatus* laccase genes. *Appl. Microbiol. Biotechnol.* **2013**, *97* (2), 705−717.

(23) Schlosser, D.; Grey, R.; Fritsche, W. Patterns of ligninolytic enzymes in *Trametes versicolor*. Distribution of extra- and intracellular enzyme activities during cultivation on glucose, wheat straw and beech wood. *Appl. Microbiol. Biotechnol.* **1997**, *47* (4), 412−418.

(24) Chiron, S.; Minero, C.; Vione, D. Photodegradation processes of the Antiepileptic drug carbamazepine, relevant to estuarine waters. *Environ. Sci. Technol.* **2006**, *40* (19), 5977−5983.

(25) Hu, L.; Martin, H. M.; Arce-Bulted, O.; Sugihara, M. N.; Keating, K. A.; Strathmann, T. J. Oxidation of carbamazepine by Mn(VII) and Fe(VI): reaction kinetics and mechanism. *Environ. Sci. Technol.* **2009**, *43* (2), 509−515.

(26) Hübner, U.; Seiwert, B.; Reemtsma, T.; Jekel, M. Ozonation products of carbamazepine and their removal from secondary effluents by soil aquifer treatment - Indications from column experiments. *Water Res.* **2014**, *49*, 34−43.

(27) Kaiser, E.; Prasse, C.; Wagner, M.; Bröder, K.; Ternes, T. A. Transformation of oxcarbazepine and human metabolites of carbamazepine and oxcarbazepine in wastewater treatment and sand filters. *Environ. Sci. Technol.* **2014**, *48* (17), 10208−10216.

DOI: 10.1021/acs.est.5b02222
Environ. Sci. Technol. 2015, 49, 12351−12362

(28) McDowell, D. C.; Huber, M. M.; Wagner, M.; Von Gunten, U.; Ternes, T. A. Ozonation of carbamazepine in drinking water: Identification and kinetic study of major oxidation products. *Environ. Sci. Technol.* **2005**, *39* (20), 8014−8022.
(29) Larraya, L. M.; Perez, G.; Penas, M. M.; Baars, J. J. P.; Mikosch, T. S. P.; Pisabarro, A. G.; Ramirez, L. Molecular karyotype of the white rot fungus *Pleurotus ostreatus*. *Appl. Environ. Microbiol.* **1999**, *65* (8), 3413−3417.
(30) Salame, T. M.; Knop, D.; Levinson, D.; Mabjeesh, S. J.; Yarden, O.; Hadar, Y. Inactivation of a *Pleurotus ostreatus* versatile peroxidase-encoding gene (mnp2) results in reduced lignin degradation. *Environ. Microbiol.* **2014**, *16* (1), 265−277.
(31) Seiwert, B.; Golan-Rozen, N.; Weidauer, C.; Riemenschneider, C.; Chefetz, B.; Hadar, Y.; Reemtsma, T., Electrochemistry Combined with LC−HRMS: Elucidating Transformation Products of the Recalcitrant Pharmaceutical Compound Carbamazepine Generated by the White-rot Rot Fungus *Pleurotus ostreatus*. *Environ. Sci. Technol.* **2015**, accepted DOI: 10.1021/acs.est.5b02229.
(32) Bu, H. Z.; Kang, P.; Deese, A. J.; Zhao, P.; Pool, W. F. Human in vitro glutathionyl and protein adducts of carbamazepine-10,11-epoxide, a stable and pharmacologically active metabolite of carbamazepine. *Drug Metab. Dispos.* **2005**, *33* (12), 1920−1924.
(33) Tybring, G.; von Bahr, C.; Bertilsson, L.; Collste, H.; Glaumann, H.; Solbrand, M. Metabolism of carbamazepine and its epoxide metabolite in human and rat liver *in vitro*. *Drug Metab. Dispos.* **1981**, *9* (6), 561−564.
(34) Grigoriev, I. V.; Nikitin, R.; Haridas, S.; Kuo, A.; Ohm, R.; Otillar, R.; Riley, R.; Salamov, A.; Zhao, X.; Korzeniewski, F.; Smirnova, T.; Nordberg, H.; Dubchak, I.; Shabalov, I. MycoCosm portal: gearing up for 1000 fungal genomes. *Nucleic Acids Res.* **2014**, *42* (D1), D699−D704.
(35) Valli, K.; Wariishi, H.; Gold, M. H. Degradation of 2,7-dichlorodibenzo-para-dioxin by the lignin degrading basydiomycete *Phanerochaete crysosporium*. *J. Bacteriol.* **1992**, *174* (7), 2131−2137.
(36) Pearce, R. E.; Uetrecht, J. P.; Leeder, J. S. Pathways of carbamazepine bioactivation in vitro: II. The role of human cytochrome p450 enzymes in the formation of 2-hydroxyiminostilbene. *Drug Metab. Dispos.* **2005**, *33* (12), 1819−1826.
(37) Kawashima, K.; Ishiguro, T. Reactions of dibenz[B,F]oxireno-[D]azepine derivatives. *Chem. Pharm. Bull.* **1978**, *26* (3), 951−955.
(38) Li, J.; Dodgen, L.; Ye, Q.; Gan, J. Degradation kinetics and metabolites of carbamazepine in soil. *Environ. Sci. Technol.* **2013**, *47* (8), 3678−3684.
(39) Mathieu, O.; Dereure, O.; Hillaire-Buys, D. Presence and ex vivo formation of acridone in blood of patients routinely treated with carbamazepine: exploration of the 9-acridinecarboxaldehyde pathway. *Xenobiotica* **2011**, *41* (2), 91−100.
(40) Furst, S. M.; Sukhai, P.; McClelland, R. A.; Uetrecht, J. P. Covalent Binding of Carbamazepine Oxidative Metabolites to Neutrophiles. *Drug Metab. Dispos.* **1995**, *23* (5), 590−594.
(41) Moir, D.; Poon, R.; Yagminas, A.; Park, G.; Viau, A.; Valli, V. E.; Chu, I. The subchronic toxicity of acridine in the rat. *J. Environ. Sci. Health, Part B* **1997**, *32* (4), 545−564.
(42) Parkhurst, B. R.; Bradshaw, A. S.; Forte, J. L.; Wright, G. P. The chronic toxicity to *Daphnia magna* of acridine, a representative azaarene present in synthetic fossil-fuel products and wastewater. *Environ. Pollut., Ser. A* **1981**, *24* (1), 21−30.
(43) McMurtrey, K. D.; Knight, T. J. Metabolism of acridine by rat-liver enzymes. *Mutat. Res. Lett.* **1984**, *140* (1), 7−11.
(44) Kosjek, T.; Andersen, H. R.; Kompare, B.; Ledin, A.; Heath, E. Fate of carbamazepine during water treatment. *Environ. Sci. Technol.* **2009**, *43* (16), 6256−6261.
(45) Gao, J.; Ellis, L. B. M.; Wackett, L. P. The University of Minnesota Biocatalysis/Biodegradation Database: improving public access. *Nucleic Acids Res.* **2010**, *38*, D488.
(46) Tixier, C.; Singer, H. P.; Oellers, S.; Muller, S. R. Occurrence and fate of carbamazepine, clofibric acid, diclofenac, ibuprofen, ketoprofen, and naproxen in surface waters. *Environ. Sci. Technol.* **2003**, *37* (6), 1061−1068.
(47) Zhang, Y. J.; Geissen, S. U.; Gal, C. Carbamazepine and diclofenac: removal in wastewater treatment plants and occurrence in water bodies. *Chemosphere* **2008**, *73* (8), 1151−1161.
(48) Goldstein, M.; Shenker, M.; Chefetz, B. Insights into the uptake processes of wastewater-born pharmaceuticals by vegetables. *Environ. Sci. Technol.* **2014**, *48* (10), 5593−5600.
(49) Malchi, T.; Maor, Y.; Tadmor, G.; Shenker, M.; Chefetz, B. Irrigation of root vegetables with treated wastewater: Evaluating uptake of harmaceuticals and the associated human health risks. *Environ. Sci. Technol.* **2014**, *48* (16), 9325−9333.
(50) Almeida, A.; Calisto, V.; Esteves, V. I.; Schneider, R. J.; Soares, A. M. V. M; Figueira, E.; Freitas, R. Presence of the pharmaceutical drug carbamazepine in coastal systems: Effects on bivalves. *Aquat. Toxicol.* **2014**, *156*, 74−87.
(51) Backhaus, T. Medicines, shaken and stirred: a critical review on the ecotoxicology of pharmaceutical mixtures. *Philos. Trans. R. Soc., B* **2014**, *369* (1656), 20130585.
(52) Jarvis, A. L.; Bernot, M. J.; Bernot, R. J. The effects of the psychiatric drug carbamazepine on freshwater invertebrate communities and ecosystem dynamics. *Sci. Total Environ.* **2014**, *496*, 461−470.
(53) Prosser, R. S.; Sibley, P. K. Human health risk assessment of pharmaceuticals and personal care products in plant tissue due to biosolids and manure amendments, and wastewater irrigation. *Environ. Int.* **2015**, *75*, 223−233.
(54) Miao, X. S.; Yang, J. J.; Metcalfe, C. D. Carbamazepine and its metabolites in wastewater and in biosolids in a municipal wastewater treatment plant. *Environ. Sci. Technol.* **2005**, *39* (19), 7469−7475.
(55) Reemtsma, T.; Weiss, S.; Mueller, J.; Petrovic, M.; Gonzalez, S.; Barcelo, D.; Ventura, F.; Knepper, T. P. Polar pollutants entry into the water cycle by municipal wastewater: A European perspective. *Environ. Sci. Technol.* **2006**, *40* (17), 5451−5458.
(56) Ternes, T. A. Occurrence of drugs in German sewage treatment plants and rivers. *Water Res.* **1998**, *32* (11), 3245−3260.
(57) Baldrian, P. Wood-inhabiting ligninolytic basidiomycetes in soils: Ecology and constraints for applicability in bioremediation. *Fungal Ecology* **2008**, *1*, 4−12.
(58) Harms, H.; Schlosser, D.; Wick, L. Y. Untapped potential: exploiting fungi in bioremediation of hazardous chemicals. *Nat. Rev. Microbiol.* **2011**, *9* (3), 177−192.

DOI: 10.1021/acs.est.5b02222
Environ. Sci. Technol. 2015, 49, 12351−12362